J Therm Anal Calorim (2016) 125:1079–1086
DOI 10.1007/s10973-016-5357-2

Characterization of composites containing $NiAl_2O_4$ spinel phase from Al_2O_3/NiO and Al_2O_3/Ni systems

Justyna Zygmuntowicz[1] · Paulina Wiecińska[2] · Aleksandra Miazga[1] · Katarzyna Konopka[1]

Received: 14 October 2015 / Accepted: 16 February 2016 / Published online: 3 March 2016

Abstract This paper focused on the characterization of the composites containing nickel aluminate spinel from Al_2O_3/NiO and Al_2O_3/Ni systems. The composites were prepared by die pressing of powders and subsequent sintering of green bodies in air atmosphere. Composites were characterized by XRD, SEM, EDS and DTA/TG/MS analyses. The physical properties of the composites were measured by Archimedes method. Quantitative description of the composites microstructure was made on the basis of SEM images using computer image analysis. The XRD studies and SEM observations of composites confirmed the presence of two phases Al_2O_3 and $NiAl_2O_4$ in the whole volume of samples from both systems. Spinel phase was evenly distributed throughout the volume of the material. Morphology of $NiAl_2O_4$ obtained from both systems was characterized by the presence of voids. The DTA/TG/MS measurements showed the characteristics of organic binder decomposition and type of gases released to the atmosphere during thermal treatment. Moreover, the DTA/TG analysis showed the temperature of spinel-phase formation for both systems. It was found that the spinel-phase $NiAl_2O_4$ formation retards the process of densification. Therefore, it can be concluded that densification of samples with spinel phase depends mainly on the volume of spinel phase in composite material and does not depend on the substrates used to prepare spinel phase. The values of the selected properties of Al_2O_3–Ni- and Al_2O_3–NiO-based materials confirmed that the physical properties depend on the type of substrates used in the fabrication of composites. The type of powder influences the open porosity of samples. For composites produced using NiO powder, open porosity is lower than for samples formed with nickel powder.

Keywords Al_2O_3–NiO · Al_2O_3–Ni · Spinel-phase $NiAl_2O_4$ · DTA/TG/MS analyses

Introduction

In the past few years, the use of composite materials has significantly increased in various applications due to the unique characteristics of these materials in comparison with metals, ceramics or polymers. The composites containing spinel phase are characterized by stability in high temperature, chemical resistance, abrasion resistance and high hardness [1–3]. A particular type of such materials is composites from Al_2O_3–Ni and Al_2O_3–NiO systems with spinel-phase $NiAl_2O_4$. The composites containing spinel phase are widely used due to their unique properties. Moreover, in the last few years they are the subject of many studies. For example, the composites $NiAl_2O_4/Al_2O_3$ are applied as structural ceramic materials [4]. Composites with the nickel aluminate phase ($NiAl_2O_4$) are also used as catalysts or precatalysts for steam reforming or as electrode materials in high-temperature fuel cells due to their unusual conductivity [4]. Composites with nickel aluminate phase can be prepared by several methods, such as a powder technique [5], sol–gel method [6–9], wet chemical methods such as hydrothermal and solvothermal methods [10], powder coating process [11], conventional impregnation

✉ Justyna Zygmuntowicz
justyna.zygmuntowicz@inmat.pw.edu.pl

[1] Faculty of Materials Science and Engineering, Warsaw University of Technology, 141 Woloska St., 02-507 Warsaw, Poland

[2] Faculty of Chemistry, Warsaw University of Technology, 3 Noakowskiego St., 00-664 Warsaw, Poland

solid-state reaction [12]. The formation of the spinel depends on many factors, e.g., time, temperature, starting substrates used in the process, and it is not still fully described. On the basis of literature data, it was found that the most important factor to generate spinel phase is sintering atmosphere [13–16]. During sintering in an oxygen environment, Ni or NiO particles can react with Al_2O_3 to form spinel. The reaction of spinel-phase $NiAl_2O_4$ formation is according to the following equation:

$Al_2O_3 + Ni + ½\ O_2 \rightarrow NiAl_2O_4$, which proceeds in two steps.

I step: $2\ Ni + O_2 \rightarrow 2\ NiO$

II step: $NiO + Al_2O_3 \rightarrow NiAl_2O_4$.

The use of NiO powder allows to bypass the stage of oxidation of Ni to NiO.

As reported by the literature and own research, the spinel phase influences the mechanical properties of composite and therefore it is important to characterize spinel distribution and its morphology [13, 15, 17–19]. For this reason, the presented research was focused on the characterization of the composites containing $NiAl_2O_4$ spinel phase from Al_2O_3/NiO and Al_2O_3/Ni system.

The aim of the present study was to characterize nickel aluminate spinel in the composites obtained from Al_2O_3–NiO and Al_2O_3–Ni systems. Composites were characterized by XRD, SEM, EDS and DTA/TG/MS and stereological analyses.

Experimental

In the experiment, the following powders were used: α-Al_2O_3 TM-DAR from Taimei Chemicals (Japan) of average particle size 133 ± 30 nm and density 3.96 g cm^{-3}, NiO powder from Alfa Aesar (USA) of average particle size 5 μm and density 6.67 g cm^{-3}, as well as Ni powder from Sigma-Aldrich (Poland) of average particle size 8.5 μm and density 8.9 g cm^{-3}. The purity of the powders was as follows: α-Al_2O_3—99.99 %, nickel oxide—99.96 % and nickel—99.99 %. Figure 1 presents SEM images of the starting powders. It was found that they were firmly agglomerated.

The composites were prepared from the powder mixtures containing 90 vol% of Al_2O_3 and 10 vol% of NiO or Ni powder. Two series of samples were prepared: series I with the addition of NiO and series II with the addition of Ni. The use of NiO powder in series I allowed to bypass the stage of oxidation of Ni to NiO before the formation of $NiAl_2O_4$ spinel phase.

The powder mixtures were homogenized in ethanol in a planetary ball mill with a rotating speed of 300 rpm for 60 min. The next step was drying at 40 °C for 48 h.

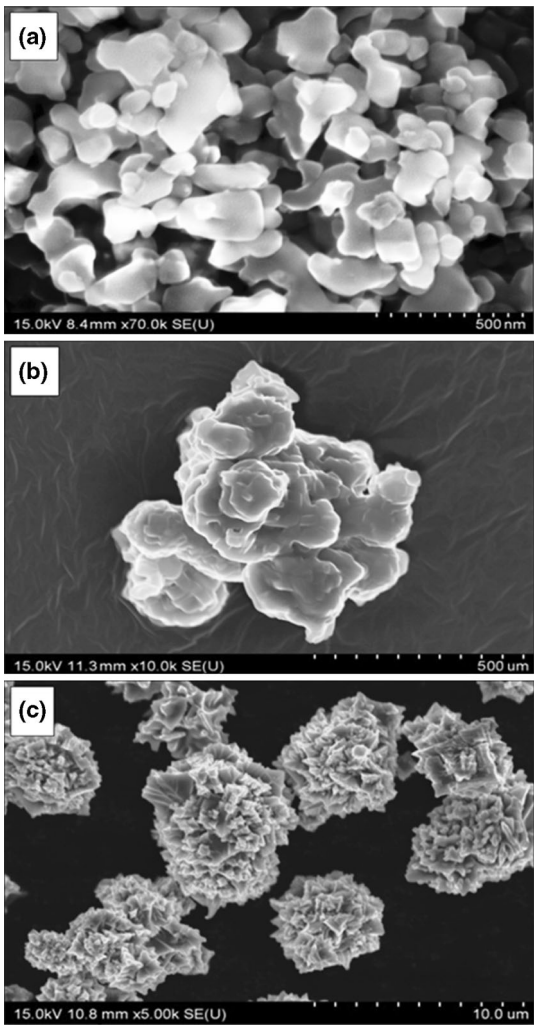

Fig. 1 SEM images of starting powders: **a** α-Al_2O_3, **b** NiO, **c** Ni

Subsequently, the poly(vinyl alcohol) (PVA) was added to the powders as a binder, and granulation was made. Then, the samples were prepared by uniaxial pressing at a pressure of 100 MPa. The dimensions of cylindrical samples were as follows: diameter $d = 20$ mm and height $h = 3$ mm. The samples were sintered in air atmosphere at temperature of 1400 °C. Dwell time was 2 h. The heating rate and cooling rate were 5 °C min^{-1}.

X-ray diffraction (XRD) was used to identify the phases present in the samples. The structural studies were carried out by using a Rigaku MiniFlex II for 2θ values ranging from 10° to 80° and using CuK$\alpha_{1.54}$ radiation and $\lambda = 1.54178$ Å. The analyses were performed at the cross sections of samples.

DTA/TG measurements were taken by using Netzsch STA 449C coupled with Quadrupole Mass Spectrometer Netzsch QMS 403C. The heating rate was 5 °C min^{-1}, and the final temperature was 1400 °C. The measurements were taken in the constant flow of two gases: argon

10 mL min^{-1} (protective gas) and synthetic air (80:20 N_2:O_2) 60 mL min^{-1}. Mass spectrometer was set to detect m/z values in mass range 10–300.

The density of obtained composites was measured by the Archimedes method according to the PN-76/E-06307. The average values were calculated from measurements of 30 samples in each series. Additionally, the densities of the sintered bodies were determined on helium pycnometer AccuPyc II 1340 (Micromeritics), in a sequence of 100 purges and 100 measurement cycles. The shrinkage after sintering process was also determined.

The microstructure of the longitudinal section of sintered specimens was investigated by scanning electron microscope Hitachi S-3500N and SU-70. The longitudinal sections were prepared by cutting the samples along the axial direction with diamond saw and then polishing with diamond paste 1 μm.

Quantitative description of the microstructure of the composites was made on the basis of SEM images of randomly selected areas on the longitudinal sections using computer image analyzer [17, 20]. The quantitative and stereological analysis was not performed for distinguished grains, but concerned the characteristics of the spinel areas (spinel particles). The distinction of spinel areas was executed on the basis of the differences in BSE contrast of $NiAl_2O_4$ and Al_2O_3 phases. The object of the study was to use the stereological analysis to determine the volume fraction of spinel phase in the composites. Moreover, based on the stereological analysis shape parameters of voids present in the spinel phase were defined: coefficient describing the elongation ($\alpha = d_{max}/d_2$), surface development ($R = p/\pi \cdot d_2$) and convexity ($W = p/p_c$) [20], where d_{max}—maximum diameter of void projection [μm], d_2—diameter of circle of the same surface as the surface of the analyzed grain [μm], p—perimeter of void [μm] and p_c—Cauchy perimeter [μm].

Results and discussion

Preliminary macroscopic observations of the composites from both series after the sintering process have shown that the samples surface was blue, which was the evidence of the presence of the spinel phase.

The X-ray diffraction patterns of samples from the series I and series II are shown in Fig. 2. For both the series, only peaks corresponding to α-alumina and cubic aluminate nickel spinel were shown in the XRD patterns. There were no changes in the alumina structure after sintering process (in comparison with initial powder). The absence of Ni and NiO peaks indicates that nickel and nickel oxide have fully reacted with alumina into nickel aluminate spinel phase. The compositions of starting powders are shown in

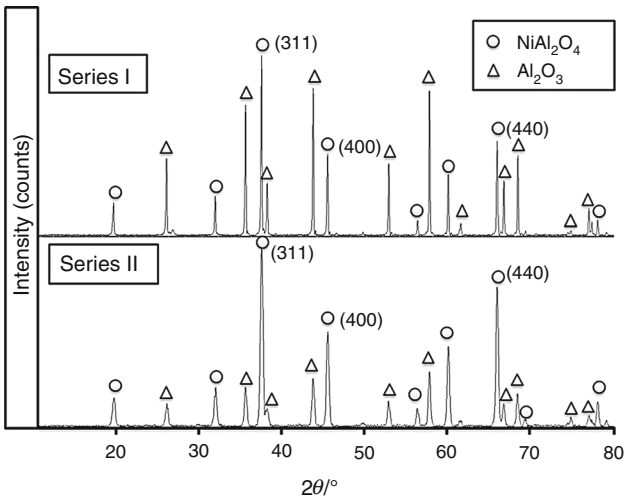

Fig. 2 XRD patterns of the Al_2O_4–$NiAl_2O_4$ composites: series I (started powders Al_2O_3 and NiO) and series II (started powders Al_2O_3 and Ni)

Table 1. Additionally, the composition of obtained sintered composite samples was calculated on the basis of the reaction stoichiometry. $NiAl_2O_4$ peaks' positions were identified by comparing with JCPDS file No. 10-0339. The major peaks for spinel were the hkl reflections of 311, 400 and 440. It was noted that the peaks of $NiAl_2O_4$ were shifted to slightly higher 2θ values as against to those of a stoichiometric $NiAl_2O_4$. This indicated that spinel in obtained sintered bodies was non-stoichiometric $NiAl_2O_4$. There was no correlation between the peak offset and the used starting powders. Moreover, the observations showed that samples from both series had sharp peaks which indicated the high crystallinity. Diffraction peaks for sample prepared from Al_2O_3/NiO mixture were slightly broadened than from Al_2O_3/Ni. It may be due to smaller crystallite size of formed spinel which results from the fact that NiO particles were smaller than nickel particles.

Thermal analysis is a useful tool to characterize the formation of spinel phases from different systems, which is reported in the literature [24, 25]. Figure 3 presents DTA/TG/DTG curves together with mass spectra for Al_2O_3/Ni green body. The endothermic peak on DTA curve with the minimum at 96 °C is visible. This peak overlaps with the peak from mass spectrometer of m/z value 18 which can be ascribed to H_2O; therefore, it indicates dehydration process. Mass spectrometer has also detected m/z value 17 of very low intensity, which confirms the presence of H_2O. The broader description concerning mass-to-charge ratio m/z for selected substances was described in previous papers [26, 27]. Then, the slight increase in intensity of m/z 18 at temperature ca. 240 °C is observed, which can be ascribed to decomposition of organic binder present in the sample. Mass spectrometer

Table 1 Composition of samples before and after sintering

Before sintering						After sintering					
Series I			Series II			Series I			Series II		
Sample	Quantity		Sample	Quantity		Sample	Quantity		Sample	Quantity	
Al_2O_3	vol%	90	Al_2O_3	vol%	90	Al_2O_3	vol%	67	Al_2O_3	vol%	42
	mol%	81		mol%	68		mol%	76		mol%	53
NiO	vol%	10	Ni	vol%	10	$NiAl_2O_4$	vol%	33	$NiAl_2O_4$	vol%	58
	mol%	19		mol%	32		mol%	24		mol%	47

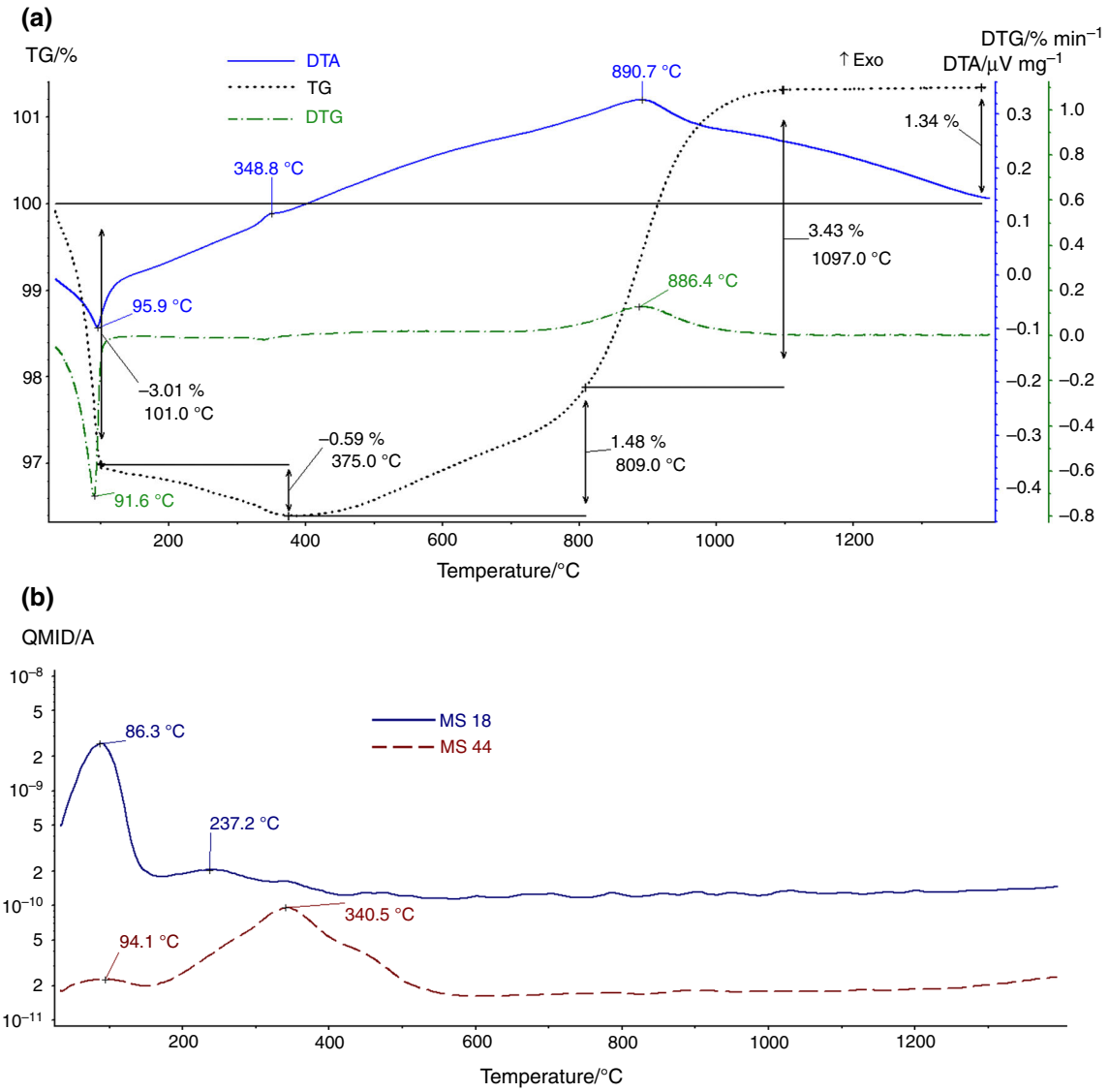

Fig. 3 DTA/TG/DTG curves (**a**) and mass spectrometer data (**b**) of Al_2O_3/Ni green bodies containing PVA

has detected also the *m*/*z* value 44 which can be ascribed to CO_2. In case of Al_2O_3/Ni, the first peak on MS 44 curve is visible at 94 °C and the second one at 341 °C. Both peaks together with mass loss on TG curve till 400 °C indicate the decomposition of polymeric binder and oxidation of decomposition products (light carbohydrates) to CO_2. The small exothermic peak at 348 °C visible only on DTA curve of Al_2O_3/Ni sample may indicate the

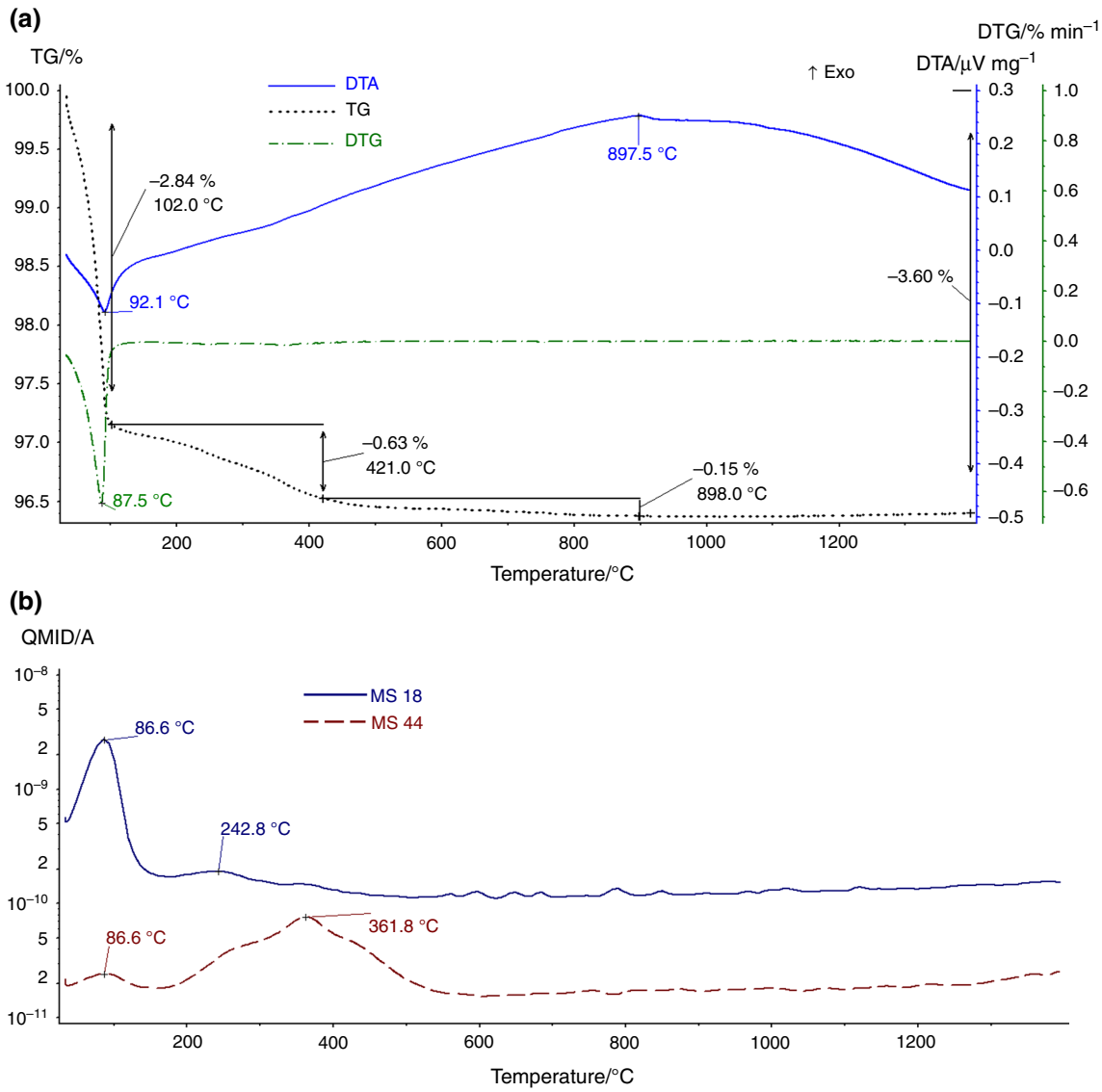

Fig. 4 DTA/TG/DTG curves (**a**) and mass spectrometer data (**b**) of Al_2O_3/NiO green bodies containing PVA

Table 2 Selected properties of composite material: series I (Al_2O_3–NiO), series II (Al_2O_3–Ni) and series III (Al_2O_3–NiO composite samples of the same composition (in mol%) as the samples of series II)

Property	Series I	Series II	Series III
Theoretical density/g cm^{-3}	4.14	4.27	4.27
Apparent density/g cm^{-3}	3.81 ± 0.03	3.43 ± 0.03	3.47 ± 0.02
Relative density/%	92.1 ± 0.9	80.3 ± 0.8	81.0 ± 0.04
Pycnometric density/g cm^{-3}	4.01 ± 0.01	4.12 ± 0.01	4.16 ± 0.01
Open porosity/%	3.54 ± 0.32	12.62 ± 0.58	8.47 ± 0.43
Linear shrinkage (samples height)/%	11.82 ± 0.16	6.28 ± 0.9	6.54 ± 0.14
Linear shrinkage (samples diameter)/%	13.56 ± 0.14	8.78 ± 0.06	8.63 ± 0.05

beginning of the oxidation of Ni to NiO. The mass loss amounting to 3.57 % is observed till 356 °C which again indicates that the first stage of thermal treatment is connected with moisture evaporation and polymer decomposition. Then, the increase in mass is observed till 1080 °C which can be ascribed to the formation of

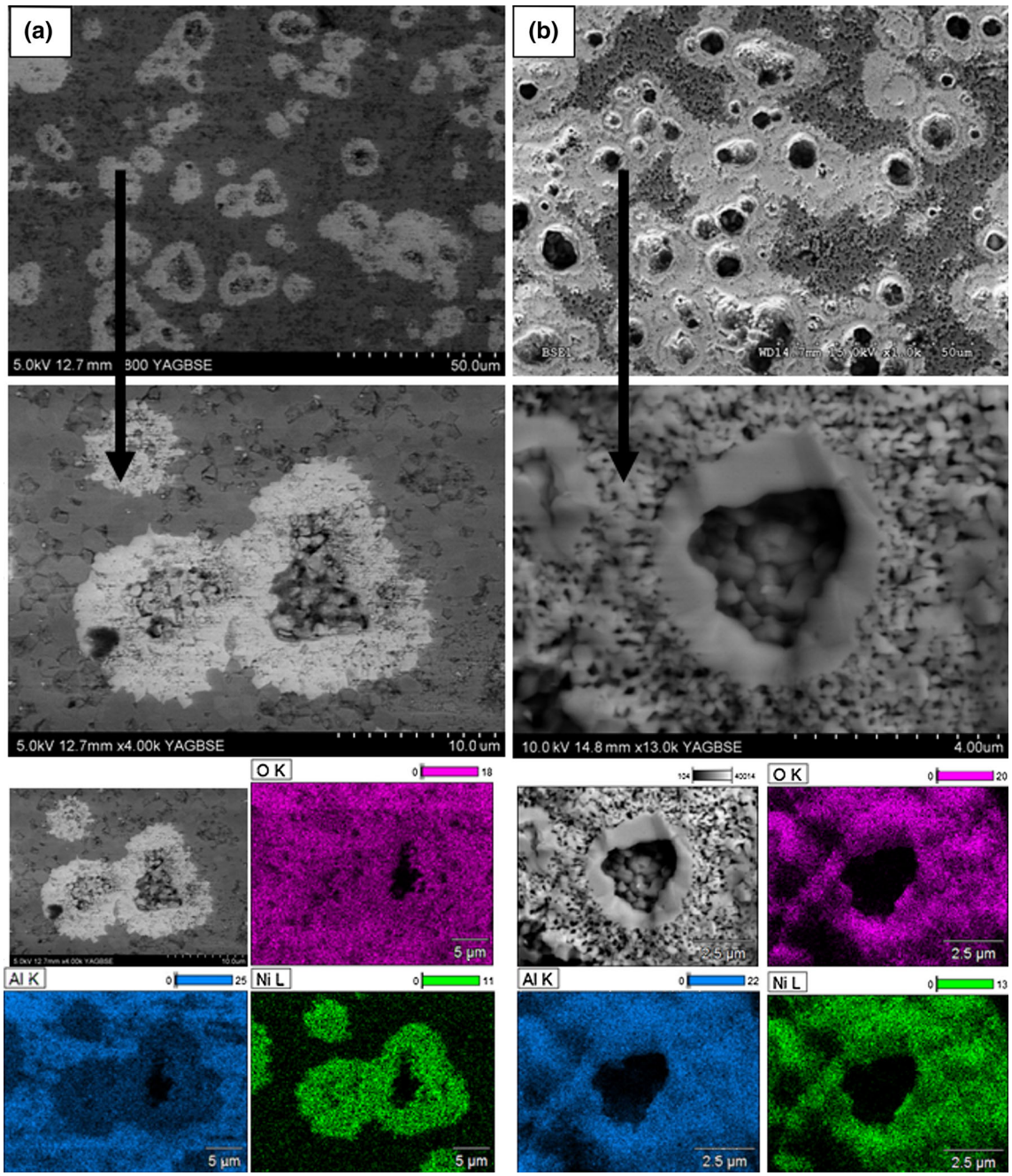

Fig. 5 SEM images of Al_2O_3–$NiAl_2O_4$ composites microstructure and chemical mapping of elements (O, Al, Ni) for selected areas: **a** series I, **b** series II

$NiAl_2O_4$ spinel phase. The mass increase in the temperature range 356–1080 °C equaled 4.91 %.

Figure 4 presents DTA/TG/DTG curves together with mass spectra for Al_2O_3/NiO green body. The total mass loss was 3.63 % which corresponds to the moisture and polymer content in the analyzed sample. The mass loss was observed till ca. 430 °C. The endothermic peak on DTA curve with the minimum at 92 °C is visible (similarly to Al_2O_3/Ni sample). This peak overlaps with the peak from mass spectrometer of *m*/*z* value 18 which indicates dehydration process. The peaks on MS 44 curve at 87 °C and the second one at 362 °C indicate the decomposition of polymeric binder.

According to DTA curves, the formation of spinel phase was observed at 891 and 897 °C, respectively, for Al_2O_3/Ni and Al_2O_3/NiO systems. At higher temperatures, the sintering process of grains proceeded. The slight difference in reaction temperature between NiO- and Ni-based samples

(7 °C) can be caused by the difference in particles size between nickel oxides; the NiO resulting from Ni oxidation is of smaller particles size than NiO used as starting material. According to the literature, the smaller the particles size, the slightly lower the reaction temperature [25].

Selected physical properties of the composites are presented in Table 2. The theoretical density was calculated according to the rule of mixtures. Calculations were made for the composition listed in Table 1. The following densities were used: 3.96 g cm^{-3} for Al_2O_3 and 4.51 g cm^{-3} for $NiAl_2O_4$ (based on JCPDS file No. 10-0339). It was found that in the case of the series II, the relative density is significantly lower than in case of series I. Moreover, the open porosity is about 3 times higher than in series I. In order to determine whether the type of substrate affects the density and shrinkage of the composite with spinel, a comparative series of samples from the Al_2O_3–NiO system was made. A composition (mol%) of comparative samples was the same as the samples of series II. Selected physical properties have shown that density and shrinkage of composites from series II and III are of the same order of magnitude. These results confirmed the fact that the spinel-phase formation retards the process of densification [20–22]. Therefore, it can be concluded that densification of samples with spinel phase depends mainly on the volume of spinel phase in composites and does not depend on the substrates used to obtain the spinel phase. The type of powder influences the open porosity of samples. For composites produced using NiO powder, open porosity is lower than for samples formed with nickel powder. This was also confirmed by pycnometric measurements. This difference may also result from the smaller particle size of NiO than that of Ni.

Nevertheless, the aim of the conducted research was to produce spinel phase from initial NiO or Ni powders. It was observed that the linear shrinkage for series I (11.82 % regarding samples height) is higher than for series II (6.28 % regarding samples height). It is in good agreement with the relative density values, because the higher the density, the higher the sintering shrinkage. Figure 5 shows the SEM micrographs of the fracture of the obtained composites. The SEM observations of the microstructure confirmed that the composite specimens were homogenous. There were no visible cracks in each series. In both, it was observed that the $NiAl_2O_4$ is characterized by two forms: the full oval shape of spinel phase and the spinel-phase areas with characteristic voids (shape of "doughnuts"). The literature reports that the shape of $NiAl_2O_4$ may result from the differences in the values of the thermal expansion coefficient and diffusion coefficient of components [15, 23].

The volume fraction of the spinel phase in composites was determined by stereological analysis. Series II had a higher value of the volume fraction (61.6 %) of the $NiAl_2O_4$ spinel phase than that of series I (30.71 %). The size of spinel grains was calculated with regard to voids present in the middle part of the spinel. For series I, the diameter (d_2) of voids (4.09 ± 0.46 μm) is slightly smaller than for series II (5.65 ± 0.57 μm). The values of parameters describing shape showed that the voids present in the spinel areas are spherical. A higher value of the variation coefficient was obtained for the series I ($\alpha = 1.48$) than for series II ($\alpha = 1.33$). The results obtained through the quantitative description of voids present in the spinel areas showed that curvature of grain boundary and convexity had the same value (for series I: $R = 1.21$ and $W = 1.01$, whereas for series II $R = 1.15$ and $W = 1.08$). It showed that the voids in the both series have similar shape. The SEM images give also the confirmation that the sintered bodies are not fully densified. Nevertheless, the determination of sintering conditions of samples containing spinel phase requires separate research.

Conclusions

Sintering of green bodies obtained from Ni or NiO and Al_2O_3 powders in the air atmosphere leads to homogeneous distribution of $NiAl_2O_4$ spinel phase in Al_2O_3 matrix. There was no delamination at the interface of $NiAl_2O_4$/Al_2O_3.

According to DTA/TG/MS analysis, spinel phase is formed at 891 and 897 °C, respectively, for Al_2O_3/Ni and Al_2O_3/NiO systems. The oxidation Ni to NiO was observed as mass increase on TG curve. Mass spectrometer allowed to observe that H_2O and CO_2 are released to the atmosphere as the products of thermal decomposition of polymeric binder used in die pressing of samples.

It was observed in each series that the spinel phase is characterized by two forms: the full oval shape of spinel phase and spinel with characteristic void inside. The results obtained through the quantitative description of voids present in the spinel areas have shown that voids have similar spherical shape. Further, it was found that the spinel-phase $NiAl_2O_4$ formation retards the process of densification in both series.

Acknowledgements This work was financially supported by the Faculty of Material Science and Engineering Warsaw University of Technology (statute work). The authors thank Professor M. Szafran and his group from the Faculty of Chemistry, Warsaw University of Technology for the scientific support.

References

1. Zengbin Y, Chuanzhen H, Bin Z, Hanlian L, Hongtao Z, Jun W. Effects of particulate metallic phase on microstructure and mechanical properties of carbide reinforced alumina ceramic tool materials. Ceram Int. 2014;40:2809–17.
2. Wachtman JB. Mechanical properties of ceramics. New York: Wiley; 1996.
3. Konopka K, Maj M, Kurzydłowski KJ. Studies of the effect of metal particles on the fracture toughness of ceramic matrix composites. Mater Charact. 2003;51:335–40.
4. Nathan TJ, Pottebaum AJ, Uz V, Laine RM. The bottom up approach is not always the best processing method: dense α-Al_2O_3/$NiAl_2O_4$ composites. Adv Funct Mater. 2014;24:3392–8.
5. Zhang X, Lu G, Hoffmann MJ, Metselaar R. Properties and interface structure of Ni and Ni–Ti alloy toughened Al_2O_3 ceramic composites. J Eur Ceram Soc. 1995;15:225–32.
6. Jeevanandam P, Koltypin Y, Gedanken A. Preparation of nanosized nickel aluminate spinel by a sonochemical method. Mater Sci Eng, B. 2002;90:125–32.
7. Rodeghiero ED, Tse OK, Giannelis EP. Interconnected metal-ceramic composites by chemical means. J Metall. 1995;47:26–8.
8. Breval E, Deng Z, Chiou S, Pantano CG. Sol–gel prepared Ni–alumina composite materials, part 1, microstructure and mechanical properties, part 1, microstructure and mechanical properties. J Mater Sci. 1992;27:26–8.
9. Cui H, Marcos Z, Levy D. A sol–gel route using propylene oxide as a gelation agent to synthesize spherical $NiAl_2O_4$ nanoparticles. J Non-Cryst Solids. 2005;35:12102–6.
10. Zhou F, Zhao X, Yuan C, Li L. Vanadium pentoxide nanowires: hydrothermal synthesis, formation mechanism, and phase control parameters. Cryst Growth Des. 2008;8:723–7.
11. Tuan WH, Wu HH, Yang TJ. The preparation of Al_2O_3/Ni composites by a powder coating technique. J Mater Sci. 1995;30:855–9.
12. Van der Laag NJ, Snel MD, Magusin PCMM, With G. Structural elastic, thermophysical and dielectric properties of zinc aluminate. J Eur Ceram Soc. 2004;24:2417–24.
13. Tuan WH, Wu HH, Chen RZ. Effect of sintering atmosphere on the mechanical properties of Ni/Al_2O_3 composites. J Eur Ceram Soc. 1997;17:735–41.
14. Tuan WH, Lin MC. Reaction sintering of Al_2O_3/$NiAl_2O_4$ composites. J Mater Sci Lett. 1996;15:735–7.
15. Zygmuntowicz J, Miazga A, Konopka K. Morphology of nickel aluminate spinel ($NiAl_2O_4$) formed in the Al_2O_3–Ni composite system sintered in air. Compos Theory Pract. 2014;14(2):106–10.
16. Halevy I, Dragoi D, Ustundag E, Yue AF, Arredondo EH, Hu J, Somayazulu MS. The effect of pressure on the structure of $NiAl_2O_4$. J Phys: Condens Matter. 2002;14:10511–6.
17. Sekino T, Nihara K. Fabrication and mechanical properties of fine-tungsten-dispersed alumina-based composites. J Mater Sci. 1997;32:3943–9.
18. Lieberthal M, Kaplan WD. Processing and properties of Al_2O_3 nanocomposites reinforced with sub-micron Ni and $NiAl_2O_4$. Mater Sci Eng, A. 2001;302:83–91.
19. Bolt PH, Lobner SF, Geus JW, Habraken FHPM. Interfacial reaction of NiO with Al_2O_3 (1120) and polycrystalline α-Al_2O_3. Appl Surf Sci. 1995;89:339–49.
20. Michalski J, Wejrzanowski T, Pielaszek R, Konopka K, Łojkowski W, Kurzydłowski KJ. Application of image analysis for characterization of powders. Mater Sci Poland. 2005;23:79–86.
21. Konopka K. Nickel aluminate spinel ($NiAl_2O_4$) in Al_2O_3-Ni composites. Inżynieria Materiałowa. 2010;3(175):457–9.
22. Tuan WH, Wu MCHH. Preparation of Al_2O_3/Ni composites by pressureless sintering in H_2. Ceram Int. 1995;21:221–5.
23. Konopka K, Lityńska-Dobrzańska L, Dutkiewicz J. SEM and TEM studies of $NiAl_2O_4$ spinel chase distribution in alumina matrix. Arch Metall Mater. 2013;58(2):501–4.
24. Queiroz RM, Coelho TL, Queiroz IM, Pires LHO, Santos IMG, Zamian JR, da Rocha Filho GN, da Costa CEF. Structural and thermal characterization of $Ni_xZn_{1-x}Al_2O_4$ synthesized by the polymeric precursor method. J Therm Anal Calorim. 2015;. doi:10.1007/s10973-015-5056-4.
25. Sepelak V, Heitjans P, Becker KD. Nanoscale spinel ferrites prepared by mechanochemical route: thermal stability and size dependent magnetic properties. J Therm Anal Calorim. 2007;90:93–7.
26. Bednarek P, Szafran M. Thermal decomposition of monosaccharides derivatives applied in ceramic gelcasting process investigated by the coupled DTA/TG/MS analysis. J Therm Anal Calorim. 2012;109:773–82.
27. Wiecinska P. Thermal degradation of organic additives used in colloidal shaping of ceramics investigated by the coupled DTA/TG/MS analysis. J Therm Anal Calorim. 2015;. doi:10.1007/s10973-015-5075-1.